

1
2
3
4
5
6
7
8
9
10
11
12
13
14
15
16
17
18
19
20
21
22
23

**Convective mixing and high littoral production established systematic errors in the
diel oxygen curves of a shallow, eutrophic lake**

Soren Brothers^{a,*}, Garabet Kazanjian, Jan Köhler, Ulrike Scharfenberger, Sabine Hilt

Leibniz-Institute of Freshwater Ecology and Inland Fisheries, Berlin, Germany

^a Present Affiliation: School of Environmental Sciences, University of Guelph, Guelph,
Ontario, Canada

* Corresponding author: Soren Brothers (sbrother@uoguelph.ca)
School of Environmental Sciences, University of Guelph
Bovey Building, Gordon St.
Guelph, Ontario, N1G 2H1
Canada

Running Head: Diel oxygen curves method reassessment

Keywords: Diel oxygen curves, convective mixing, metabolism, primary production,
littoral.

24 **Abstract**

25 The diel (24-hour) oxygen (O₂) curves approach has become a popular method for
26 analyzing gross primary production (GPP) and ecosystem respiration (ER) rates in
27 aquatic systems. Despite the simplicity of this approach, there remain aspects of the
28 calculation and interpretation of diel O₂ curves which may skew results, with potentially
29 large implications for estimates of metabolic rates. One common problem in lakes is the
30 occurrence of unexpected changes in O₂ concentrations (for instance, increasing
31 overnight O₂ concentrations). Such changes have typically been ascribed to the random
32 mixing of pockets of O₂. It has thus been suggested that negative GPP or positive ER
33 values should be included in calculations, on the assumption that under- and
34 overestimates should occur with equal frequency, and thus cancel each other out. Our
35 data from a shallow, eutrophic lake provided a high share of negative GPP values. We
36 argue that these may have been the result of elevated littoral productivity coupled with
37 convective currents produced by consistent differences in the heating or cooling of littoral
38 and offshore waters. Such phenomena might be common in small, sheltered lakes where
39 the role of mixing by wind is diminished. We conclude that a failure to account for
40 consistent metabolic gradients and periodic convective mixing may lead to a chronic
41 underestimation of metabolic rates in lakes when using the diel O₂ curves method.

42

43

44

45

46

47 **Introduction**

48 The diel (24-hour) oxygen (O₂) curve technique has rapidly become an accepted
49 standard approach for measuring metabolic rates in aquatic ecosystems since being
50 designed for fluvial systems six decades ago (Odum, 1956). By measuring the rates at
51 which pelagic day- and nighttime O₂ concentrations change, this approach offers
52 researchers an elegant, simple way to quantify ecosystem respiration (ER) and gross
53 primary production (GPP) rates (Staehr et al., 2010; Hoellein et al., 2013). Specifically,
54 Hanson et al. (2008), adapting from Odum (1956), proposed that the areal rate of change
55 of dissolved oxygen (Q) at a given station could be calculated using the model:

56
$$Q = GPP - R + D + A \quad (1)$$

57 Where GPP is the areal rate of gross primary production, R is the areal community
58 respiration rate, D is the local flux of O₂ between the water surface and atmosphere, and
59 A represents all other O₂ fluxes, such as those resulting from vertical or horizontal
60 mixing. For rapidly-and thoroughly-mixed fluvial systems, diel O₂ curves based on single
61 probe deployments are expected to represent both benthic and water column production.
62 In lakes, the degree to which whole-lake metabolic rates can be accurately estimated
63 using the diel O₂ curves method varies with the location and duration of an O₂ probe's
64 installation, the rate at which a lake's water column is mixed, and the metabolic
65 variability within a given mixed layer (Van de Bogert et al., 2012; Obrador et al., 2014).
66 Calculated GPP values might therefore only represent phytoplankton production rates
67 within the measured mixed layer, and the degree of benthic and littoral periphyton
68 (attached algae) or macrophyte contribution would increase with water mixing and/or
69 measuring proximity to those environments (Coloso et al., 2008). Considering the

70 potentially large variations in metabolic rates between the water column, benthos, and
71 littoral zones of a given lake, the chosen measurement location may influence the
72 resulting data (Lauster et al. 2006; Caraco and Cole 2002; Van de Bogert et al., 2007;
73 Sadro et al., 2011; Staehr et al., 2012). Littoral macrophyte beds can boost net ecosystem
74 production (NEP), producing high dissolved O₂ concentrations in the littoral surface
75 waters compared to offshore surface waters (Unmuth et al., 2000; Lauster et al., 2006;
76 They et al., 2013; Idrizaj et al. 2016; Fig. 1).

77 With rapid and/or random mixing of lake waters, elevated littoral primary
78 productivity rates might influence long-term offshore O₂ curves. However, during low-
79 wind periods or sheltered conditions, convective currents created by differences in
80 nighttime cooling or daytime heating rates between the shallow littoral zone and deeper
81 offshore zone may come to dominate lake circulation patterns (Horsch and Stefan, 1988;
82 MacIntyre and Melack, 1995; Forrest et al., 2008; Fig. 1). Such convective forces may
83 produce both horizontal and vertical penetrative currents, and are usually associated with
84 the summer and winter months (Forrest et al., 2008; Salonen et al., 2014). Summertime
85 littoral-to-offshore flow rates have been measured from 4 to 20 m h⁻¹ (James and Barko,
86 1991), while littoral flushing periods have been estimated of one to four hours, varying
87 with macrophyte cover (Oldham and Sturman, 2001). The regular occurrence of such
88 convective currents, coupled with typically elevated daytime O₂ production in the littoral
89 zone (relative to the off-shore water column), could feasibly result in a nightly recurrent
90 bias whereby nighttime O₂ concentrations increase at off-shore sites in lakes, producing
91 negative metabolic values (Fig. 2). Similarly, elevated littoral O₂ depletion at night could
92 result in a supply of O₂-depleted water to the lake center the following day, with the same

93 outcome for calculated metabolic rates (Fig. 2). Such impossible negative GPP values
94 have been reported when applying this method to lakes, though it has been suggested that
95 they are likely the result of the random mixing of pockets of high and low dissolved O₂ in
96 the water column, or term “A” in Eq. 1 (Staeher et al., 2010). It has therefore been
97 assumed that underestimated values, which we here consider to be (metabolically
98 impossible) negative GPP values calculated from low daytime NEP or positive calculated
99 ER rates (i.e. oxygen concentrations increasing overnight absent primary production),
100 occur as frequently as overestimated values, with the suggested solution being that all
101 values be included in the calculations of mean metabolic rates (Staeher et al., 2010).

102 In this study, we analyzed diel O₂ curves and concurrent independent
103 phytoplankton GPP measurements from a small, shallow temperate lake to examine the
104 frequency, seasonality, and severity of GPP rates that were calculated to be negative. We
105 predicted that convective mixing coupled with higher littoral GPP may introduce a
106 systematic bias into our estimated metabolic rates. Such bias could be especially
107 significant when applying the diel O₂ curve method to embayments or small, sheltered
108 lakes with high littoral-to-pelagic ratios, where convective mixing may play a large role.
109 A re-evaluation of the applicability of the diel O₂ curves method for metabolic rates in
110 small lakes could have broader implications for global estimates of metabolism in aquatic
111 ecosystems. New research has documented that lakes play an important role in regional
112 and global carbon cycling (Tranvik et al., 2009). Furthermore, most lakes have surface
113 areas less than 1 km² and are often characterized by a high percentage of lake area
114 occupied by the littoral zone, and possibly a high degree of sheltering from wind (for
115 instance, by surrounding trees), and thus present a greater potential role for convective

116 mixing (Downing et al., 2006; Verpoorter et al., 2014). It is thus important to determine
117 whether such a bias exists, and to quantify how severe it might be.

118

119 **Materials and procedures**

120 We present data from Schulzensee (53°14'N, 13°16'E), a small (3 ha, radius = ~
121 100 m), shallow, eutrophic lake (mean total phosphorus concentration in 2010: $34 \pm 3 \mu\text{g}$
122 L^{-1}) located in a rural lowland area of northeastern Germany. Schulzensee's primary
123 production is provided by phytoplankton and periphyton, non-rooted submerged
124 macrophytes (primarily *Ceratophyllum submersum*) in the littoral areas during
125 summertime, and colony-forming benthic cyanobacteria (*Aphanothece stagnina*)
126 (Brothers et al., 2013a,b). Though fed by groundwater, this lake features no surface
127 inflows or outflows, and is naturally sheltered by alder trees (*Alnus glutinosa*) and located
128 in a forested depression. It is thus expected to experience only minor wind-driven
129 resuspension. Schulzensee's littoral zone occupies roughly 32% of the lake surface area,
130 and its shallow mean depth (2.2 m) resulted in a relatively large proportion (~50%) of the
131 whole-lake GPP being represented by benthic production (Brothers et al., 2013b).

132 Yellow Springs Instruments (YSI, Xylem Inc., Yellow Springs, OH, USA) sondes
133 were installed at a lake-center monitoring station from May 8th, 2010 to May 7th, 2011, at
134 a depth of approximately 1.2 m (varying with minor lake level fluxes). These sondes
135 recorded temperature, O₂, and pH every 10 minutes during the full year. YSI sondes were
136 also used to measure vertical profiles from the surface to sediments (at gradients of 0.5
137 m) every four weeks throughout the study period. GPP and ER were calculated from diel
138 O₂ curves (Eq. 1) following the procedures of Staehr et al. (2010), also known as the

139 “bookkeeping approach”. Specifically, ER was calculated as the mean change in O₂ (per
140 10 minutes) from one hour after dusk until dawn (thus typically giving it a negative sign).
141 ER was subtracted from net production (NP) rates calculated by the same methods for the
142 following day to provide GPP (typically giving it a positive sign). Diel O₂ curves were
143 corrected for atmospheric O₂ fluxes following Gelda and Effler (2002), using lake-center
144 wind speed data recorded every 10 minutes by a meteo multiprobe (ecoTech, Bonn,
145 Germany). Surface fluxes were corrected for a period of stratification (July 16th to August
146 24th) by adopting the mean measured surface O₂ concentrations from profiles to avoid
147 overestimating O₂ losses to the atmosphere. Production values are expressed in carbon
148 units applying a respiratory quotient of one. Although the fundamental assumptions of
149 our hypothesis may be considered applicable to both GPP and ER values (Fig. 1), our
150 analyses focus on calculated GPP values, since GPP was the metabolic parameter for
151 which corollary data (as phytoplankton GPP) were available. Convective mixing is
152 expected to affect daytime O₂ curves as well as nighttime ones (Fig. 1), though we here
153 focus on the phenomenon of increasing nighttime O₂ curves, which cannot be explained
154 by metabolic processes. Since daytime net production is influenced by both GPP and ER
155 concomitantly, it can feasibly be positive or negative, making the non-metabolic effects
156 of mixing on daytime curves more difficult to identify.

157 Independent calculations of pelagic (lake-center) phytoplankton GPP were made
158 from monthly measurements of chlorophyll *a* (Chl *a*) concentrations (mixed depth lake-
159 center samples, from 0.5 m, 1 m, and 2 m), fluorescence, and light attenuation (Brothers
160 et al., 2013b). Photosynthetic parameters were obtained from rapid photosynthesis-
161 irradiance (P-I) curves measured within three hours of sampling using the modular

162 version of a Phyto-PAM fluorometer (Phyto-PAM, Walz, Effeltrich, Germany) equipped
163 with a 10 mm cuvette. The concentration of Chl *a* in water samples was measured by
164 high-performance liquid chromatography (HPLC, Waters, Millford, MA, USA),
165 following Shatwell et al. (2012). Phytoplankton GPP was calculated for each 10 cm layer
166 of the water column using hourly depth-specific PAR (derived from global radiation at
167 the water surface and light attenuation of the water column), with each measurement
168 being multiplied by the estimated water volume at a specific depth. The sum of these
169 measurements was used to calculate daily whole-lake phytoplankton production
170 (Brothers et al., 2013b). Due to an anticipated minimal light transmission through heavy
171 snow and ice, phytoplankton GPP could not be reliably calculated, and was thus assumed
172 to be zero during the full period of ice cover (December 1st, 2010 to March 15th, 2011).
173 Statistical tests were made using JMP (Version 7, SAS Institute) and values are provided
174 with standard error of the mean unless otherwise specified.

175

176 **Assessment**

177 Over the course of the full study year, O₂ curves from 293 24-hour periods were
178 available for analysis. This was after accounting for sonde malfunction and two outliers,
179 which occurred during periods of potential ice break-up, during which lake surface-to-
180 atmosphere O₂ flux rates could not be established. The mean GPP rate calculated by the
181 diel O₂ curve method with negative values included (following the standard book-
182 keeping approach) was $83 \pm 21 \text{ g C m}^{-2} \text{ y}^{-1}$. When negative values were excluded, the
183 full-year mean value rose significantly to $315 \pm 22 \text{ g C m}^{-2} \text{ y}^{-1}$ (Wilcoxon Test, $p <$
184 0.0001). Independently determined phytoplankton GPP rates calculated from

185 fluorescence measurements for the same dates as available O₂ curves were 216 ± 12 g C
186 m⁻² y⁻¹ (Table 1).

187 The significant difference between GPP calculations with and without the
188 inclusion of negative values results from the abundance of such abnormal values.
189 Increasing nighttime O₂ concentrations were observed on 45% of the available dates
190 (Table 1, Fig. 3). Seasonally, these were found to occur most frequently in winter
191 (December to February; 81%), followed by summer (June to August; 40%), fall (March
192 to May; 32%) and spring (September to November; 30%). The exclusion of negative GPP
193 values significantly affected the mean calculated values for all seasons in this lake ($p <$
194 0.05, Wilcoxon Test). The severity of this effect was greatest in summer and winter
195 months (Table 1), the summer influencing annual GPP mean values to a greater extent
196 due to their lower values (minimum GPP = -2802 mg C m⁻² d⁻¹) compared to those in the
197 winter (minimum GPP = -742 mg C m⁻² d⁻¹).

198

199 **Discussion**

200 When inaccuracies in daily GPP estimates result from measurement imprecision
201 or random patterns of O₂ dispersion in the water column of a lake, underestimates and
202 overestimates in GPP rates should balance each other out, providing accurate mean
203 productivity rates over time. Based on this assumption, standard procedures suggest the
204 inclusion of negative GPP estimates and lengthy sampling periods (e.g., Staehr et al.,
205 2010). In our study lake the inclusion of negative GPP values would provide roughly four
206 times lower annual GPP rates than with negative values excluded. A comparison of these
207 values with mean phytoplankton GPP over the same sampling dates (216 ± 12 g C m⁻² y⁻¹

208 ¹) indicates that the inclusion of negative GPP values in the O₂ curves approach
209 (providing a mean of $83 \pm 21 \text{ g C m}^{-2} \text{ y}^{-1}$) is not balanced out by overestimation, and thus
210 the inclusion or exclusion of negative values leads to a systematic bias, and likely
211 introduces inaccuracies. Furthermore, the inclusion of the negative GPP values not only
212 underestimates phytoplankton GPP in this lake, but it also fails to capture any additional
213 littoral periphyton production occurring within the mixed layer. This is corroborated by a
214 regression from del Giorgio and Peters (1993), linking pelagic Chl *a* concentrations to
215 phytoplankton GPP calculated via the same methodology. Given a mean annual Chl *a*
216 concentration of $13 \mu\text{g L}^{-1}$ (from Brothers et al., 2013a), pelagic phytoplankton GPP in
217 our study lake should be approximately $175 \text{ g C m}^{-2} \text{ y}^{-1}$ (assuming a mean lake depth of
218 2.2 m).

219 For convective mixing to be the source of our observed bias, littoral oxygen
220 concentrations would need to be higher than pelagic oxygen concentrations (in order to
221 increase nighttime lake-center oxygen concentrations), and convective currents would
222 need to flow at a rate sufficient to transport water from the littoral zone to the lake center
223 within a nighttime period. The YSI sonde in our study lake was situated approximately
224 80 m from the nearest littoral zone, meaning that a flow rate of roughly 7 m h^{-1} would be
225 required for midday O₂-rich littoral waters to travel convectively to reach the probe by
226 midnight. This flow rate is well within the range of convective flow rates (4 to 20 m h^{-1})
227 described by James and Barko (1991). As part of a separate, later analysis, YSI sondes
228 (of the same model as that in our study, and both with 10-minute sampling frequencies)
229 measured littoral and pelagic O₂ concentrations simultaneously in this lake during a two-
230 week period in September 2011. They confirmed that mean O₂ concentrations were

231 significantly higher in the littoral zone ($2.66 \pm 0.03 \text{ mg L}^{-1}$ $n = 2160$) than in the pelagic
232 zone ($1.49 \pm 0.03 \text{ mg L}^{-1}$; $n = 2087$; Wilcoxon Test, $p < 0.0001$). We do not have enough
233 data to say whether this difference between habitats was a result of net metabolic
234 differences, differing rates of aeration due to wave action in the shallower depths of the
235 littoral, or the result of a somewhat shallower probe exposure depth ($\sim 0.5 \text{ m}$) in the
236 littoral zone compared to the pelagic probe ($\sim 0.8 \text{ m}$ during this later study period).
237 Forrest et al. (2008) note that summer and winter months, when shear stresses due to
238 wind have their lowest effects on temperate lakes, are the periods when convective
239 mixing plays the largest role. Notably, these were also the seasons during which our
240 study lake, as well as another similarly-sized lake in the region for which O_2 curves were
241 available (data not shown), experienced the highest frequency and strongest effect of
242 false negative GPP rates. Ice covered our study lake during the full winter period, while
243 the summer months featured the largest daily difference in air temperatures, as well as the
244 lowest wind speeds, making both seasons ideal for maximizing the effects of convective
245 mixing events on O_2 concentrations (Table 1). However, to definitively conclude that
246 convective mixing was the source of false negative GPP rates would require detailed
247 measurements of water flow rates, as well as littoral and pelagic O_2 concentrations.

248 False negative GPP rates can also be a result of other physical factors. Daily
249 microstratification dynamics, producing deeper mixing depths in the morning and
250 shallower ones in the afternoon (Coloso et al., 2011), could potentially result in periodic
251 errors if YSI sondes cross periodically between mixing zones. Although profiles revealed
252 summertime vertical O_2 concentration gradients in this lake, estimated mixing depths
253 during our study period were typically greater than 1.5 m depth (data not shown). These

254 estimates were derived from data typically collected around midday or the early
255 afternoon, suggesting that it is feasible that mixing depths in the late afternoon may be
256 lower (Coloso et al., 2011), producing sudden shifts in measured O₂ concentrations.
257 However, Tinytag temperature loggers (Gemini Data Loggers Inc, Chichester, UK)
258 installed at every 50cm depth following our study period (July 29th to October 14th, 2011)
259 detected no notable (>0.25 °C), recurrent daily shifts in temperature between one and two
260 meters below the surface, where our sonde had been located.

261 We furthermore considered the possibility that oxygen-poor groundwater entering
262 the lake may have influenced the measured diel O₂ curves. Groundwater volumetric
263 fluxes had been estimated for this lake during the same period using data taken from two
264 small wells in the immediate vicinity (four to six meters from the shore). Given the lack
265 of surface inflows or outflows to this system, monthly groundwater fluxes were
266 occasionally large, representing as much as ~6% of the full lake water volume (data not
267 shown), potentially decreasing summertime O₂ concentrations by that same fraction
268 (assuming groundwater to be anoxic). However, groundwater loading would not fluctuate
269 along a daily, periodic cycle, and thus would not be expected to influence diel O₂ curves
270 measured over a prolonged exposure period.

271 The total GPP of Schulzensee during this study year (including benthic, littoral,
272 and pelagic primary producers) was estimated by Brothers et al. (2013b) to be 550 g C m⁻²
273 y⁻¹ (one third of which was attributed to phytoplankton). It is thus feasible that positive-
274 only O₂ curve GPP rates (315 ± 22 g C m⁻² y⁻¹) provided a roughly accurate estimate of
275 mixed-layer GPP alone, assuming that benthic GPP may not have been fully mixed into
276 the surface water layer. However, as one may still anticipate false positives and false low

277 GPP values (even if they are not negative), we cannot suggest that the automatic
278 exclusion of negative GPP values will provide reliable data. Rather, the amplitude of the
279 bias from convective mixing would vary according to factors such as seasonality, plant
280 community structure, wind exposure, lake fetch and bathymetry, and O₂ probe placement.

281 We suggest that, in addition to random mixing events, periodic mixing events
282 such as convective mixing could play a major role in the physical mixing of O₂ in small
283 lakes, which could in turn negatively affect diel O₂ curve calculations. On a small-to-
284 medium timescale (days to weeks), rapid and variable changes in O₂ concentrations could
285 result from random processes such as wind-driven mixing (e.g., Cremona et al., 2014).
286 Such occurrences may be treated using “smoothing” modeling approaches (designed to
287 reduce variability), such as Bayesian models (Solomon et al., 2013; Cremona et al., 2014)
288 or Kalman filters (Batt and Carpenter, 2012). A separate analysis of our dataset using
289 multiple modeling approaches (Bayesian, bookkeeping, Kalman, maximum-likelihood
290 estimation, and ordinary least squares) provided by the R package “LakeMetabolizer”
291 (Winslow et al., 2016) reveals that the smoothing models are successful at constraining
292 the range of GPP values produced, but the overall mean GPP values do not differ
293 significantly between approaches (Wilcoxon Test, $p = 0.94$) and negative GPP values
294 remain common (Fig. 4).

295 Random mixing events (here considered any which do not occur on a regular 24-h
296 cycle) typically occur in the spring and fall, when the water column is frequently mixed
297 by low vertical temperature-driven density gradients and higher winds. However, diel
298 periodic mixing patterns are most likely to establish during summer and winter, when the
299 effects of wind on water column mixing are reduced, especially in lakes in landscape

300 depressions sheltered from the wind. Due to the periodicity of such events, models which
301 simply reduce the mixing weight (i.e. relative calculated importance) of outliers or highly
302 variable events are poorly suited to derive reliable metabolism rates during such periods.
303 Adding complexity to diel O₂ calculations also fails to enhance the accuracy of metabolic
304 calculations when processes such as internal waves, microstratification, or convective
305 currents influence the variability of O₂ in the water column (Hanson et al., 2008). We
306 therefore propose that an enhancement to Odum's (1956) fundamental calculation of diel
307 O₂ curves is needed, especially when considering small, sheltered lakes:

$$308 \quad Q = GPP - R + D + A_r + A_p + GW \quad (2)$$

309 The term "GW" has been introduced to reflect the possible role played by anoxic
310 groundwater intrusion on small lakes lacking surface in- or out-flows. The term "A",
311 which initially represented water column mixing (Eq. 1), is here divided into "A_r",
312 representing random mixing events (e.g., wind-driven mixing), and "A_p," representing
313 periodic mixing events such as convective mixing following different warming/cooling
314 regimes between nearshore and offshore waters, or daily microstratification events.
315 During spring and fall, A_r is anticipated to play an important role, and the use of
316 smoothing models such as Kalman filters (Batt and Carpenter, 2012), or the removal of
317 dates with high wind speeds or low solar irradiance (Rose et al., 2014) is recommended
318 to reduce the presence of outliers. While the effect of A_p on diel O₂ curves may be
319 greatest in summer and winter, its magnitude depends upon lake size and bathymetry,
320 changes in air temperature, and the difference between littoral and off-shore O₂
321 production, making it more difficult to predict.

322

323 **Comments and recommendations**

324 Although diel O₂ curves remain one of the most cost- and time-efficient methods
325 for calculating metabolic rates in aquatic ecosystems, we note that their utility may be
326 limited in some situations. We advise researchers to critically examine the frequency and
327 severity of false negative metabolic rates, taking into consideration possible factors which
328 could be responsible for producing them, especially if they comprise a significant share
329 of calculated rates. Although it is possible to estimate horizontal exchange flow rates
330 based on the littoral benthic slope (e.g., Sturman et al., 1999), more research (including
331 direct measurements with an acoustic Doppler current profiler) would be necessary to
332 establish whether such a calculation could provide enough information to reliably avoid
333 the common recurrence of false negative metabolic values. As a first step, we suggest that
334 researchers adopt multiple independent approaches when determining ecosystem
335 productivity. Additionally, in lakes in which periodic mixing events (A_p in Eq. 2) such as
336 convective mixing or microstratification events may occur (during summer or wintertime
337 months in shallow lakes or embayments), multiple sampling depths and distances from
338 the littoral zone during these seasons may improve the reliability of metabolism rates
339 calculated from diel O₂ curves.

340

341

342

343

344

345

346 **References**

- 347 Batt, R. D., and S. R. Carpenter. 2012. Free-water lake metabolism: addressing noisy
348 time series with a Kalman filter. *Limnol. Oceanogr. Methods* **10**: 20-30.
- 349 Brothers, S. M., S. Hilt, K. Attermeyer, and others. 2013a. A regime shift from
350 macrophyte to phytoplankton dominance enhances carbon burial in a shallow,
351 eutrophic lake. *Ecosphere* **4**: 137.
- 352 Brothers, S. M., S. Hilt, S. Meyer, and J. Köhler. 2013b. Plant community structure
353 determines primary productivity in shallow, eutrophic lakes. *Freshwater Biol.* **58**:
354 2264-2276.
- 355 Caraco, N. F., and J. J. Cole. 2002. Contrasting impacts of a native and alien macrophyte
356 on dissolved oxygen in a large river. *Ecol. Appl.* **12**: 1496-1509.
- 357 Coloso, J. J., J. J. Cole, P. C. Hanson, and M. L. Pace. 2008. Depth-integrated,
358 continuous estimates of metabolism in a clear-water lake. *Can. J. Fish. Aquat. Sci.*
359 **65**: 712-722.
- 360 Coloso, J. J., J. J. Cole, and M. L. Pace. 2011. Short-term variation in thermal
361 stratification complicates estimation of lake metabolism. *Aquat. Sci.* **73**: 305-315.
- 362 Cremona, F., A. Laas, P. Nõges, and T. Nõges. 2014. High-frequency data within a
363 modeling framework: On the benefit of assessing uncertainties of lake metabolism.
364 *Ecol. Mod.* **294**: 27-35.
- 365 del Giorgio, P. A., and R. H. Peters. 1993. Balance between phytoplankton production
366 and plankton respiration in lakes. *Can. J. Fish. Aquat. Sci.* **50**: 282-289.
- 367 Downing, J. A., Y. T. Prairie, J. J. Cole, and others. 2006. The global abundance and size
368 distribution of lakes, ponds, and impoundments. *Limnol. Oceanogr.* **51**: 2388-2397.

369 Forrest, A. L., B. E. Laval, R. Pieters, and D. S. S. Lim. 2008. Convectively driven
370 transport in temperate lakes. *Limnol. Oceanogr.* **53**: 2321–2332.

371 Gelda, R. K., and S. W. Effler. 2002. Estimating oxygen exchange across the air-water
372 interface of a hypereutrophic lake. *Hydrobiologia* **487**: 243-254.

373 Hanson, P. C., S. R. Carpenter, N. Kimura, C. Wu, S. P. Cornelius, and T. K. Kratz.
374 2008. Evaluation of metabolism models for free-water dissolved oxygen methods in
375 lakes. *Limnol. Oceanogr. Methods* **6**: 454-465.

376 Hoellein, T. J., D. A. Bruesewitz, and D. C. Richardson. 2013. Revisiting Odum (1956):
377 A synthesis of aquatic ecosystem metabolism. *Limnol. Oceanogr.* **58**: 2089–2100.

378 Horsch, G. M., and H. G. Stefan. 1988. Convective circulation in littoral waters due to
379 cooling. *Limnol. Oceanogr.* **33**: 1068-1083.

380 Idrizaj, A., A. Laas, U. Anijalg and P. Nõges 2016. Horizontal differences in ecosystem
381 metabolism of a large shallow lake. *J. Hydrol.* **535**: 93-100.

382 James, W. F., and J. W. Barko. 1991. Littoral-pelagic phosphorus dynamics during
383 nighttime convective circulation. *Limnol. Oceanogr.* **36**: 949-960.

384 Lauster, G. H., P. C. Hanson., and T. K. Kratz. 2006. Gross primary production and
385 respiration differences among littoral and pelagic habitats in northern Wisconsin
386 lakes. *Can. J. Fish. Aquat. Sci.* **63**: 1130-1141.

387 MacIntyre, S., and J. M. Melack. 1995. Vertical and horizontal transport in lakes: linking
388 littoral, benthic, and pelagic habitats. *J. N. Am. Benthol. Soc.* **14**: 599-615.

389 McNair, J. N., L. C. Gereaux, A. D. Weinke, M. R. Sesselmann, S. T. Kendall, and B. A.
390 Biddanda. 2013. New methods for estimating components of lake metabolism based
391 on free-water dissolved-oxygen dynamics. *Ecol. Mod.* **263**: 251-263.

392 Monismith, S. G., J. Imberger, and M. L. Morison. 1990. Convective motions in the
393 sidearm of a small reservoir. *Limnol. Oceanogr.* **35**: 1676-1702.

394 Obrador, B., P. A. Staehr, and J. P. C. Christensen. 2014. Vertical patterns of metabolism
395 in three contrasting stratified lakes. *Limnol. Oceanogr.* **59**: 1228-1240.

396 Odum, H. T. 1956. Primary production in flowing waters. *Limnol. Oceanogr.* **1**: 102-117.

397 Oldham, C. E., and J. J. Sturman. 2001. The effect of emergent vegetation on convective
398 flushing in shallow wetlands: Scaling and experiments. *Limnol. Oceanogr.* **46**:
399 1486-1493.

400 Rose, K. C., L. A. Winslow, J. S. Read, E. K. Read, C. T. Solomon, R. Adrian, and P. C.
401 Hanson. 2014. Improving the precision of lake ecosystem metabolism estimates by
402 identifying predictors of model uncertainty. *Limnol. Oceanogr.: Methods* **12**: 303-
403 312.

404 Sadro, S., J. M. Melack, and S. MacIntyre. 2011. Spatial and temporal variability in the
405 ecosystem metabolism of a high-elevation lake: integrating benthic and pelagic
406 habitats. *Ecosystems.* **14**: 1123-1140.

407 Salonen, K., M. Pulkkanen, P. Salmi, and R. W. Griffiths. 2014. Interannual variability of
408 circulation under spring ice in a boreal lake. *Limnol. Oceanogr.* **59**: 2121-2132.

409 Shatwell, T., A. Nicklisch, and J. Köhler. 2012. Temperature and photoperiod effects of
410 phytoplankton growing under simulated mixed layer light fluctuations. *Limnol.*
411 *Oceanogr.* **57**: 541-553.

412 Solomon, C. T., D. A. Bruesewitz, D. C. Richardson, and others. 2013. Ecosystem
413 respiration: drivers of daily variability and background respiration in lakes around
414 the globe. *Limnol. Oceanogr.* **58**: 849-866.

415 Staehr, P. A., D. Bade, M. C. Van de Bogert, and others. 2010. Lake metabolism and the
416 diel oxygen technique: State of the science. *Limnol. Oceanogr.: Methods* **8**: 628-
417 644.

418 Staehr, P. A., J. P. A. Christensen, R. D. Batt, and J. S. Read. 2012. Ecosystem
419 metabolism in a stratified lake. *Limnol. Oceanogr.* **57**: 1317-1330.

420 Sturman, J. J., C. E. Oldham, and G. N. Ivey. 1999. Steady convective exchange flows
421 down slopes. *Aquat. Sci.* **61**: 260-278.

422 They, N. H., D. da M. Marques, and R. S. Souza. 2013. Lower respiration in the littoral
423 zone of a subtropical shallow lake. *Front. Microbiol.* **3**: 434.

424 Tranvik, L., J. A. Downing, J. B. Cotner, and others. 2009. Lakes and impoundments as
425 regulators of carbon cycling and climate. *Limnol. Oceanogr.* **54**: 2298-2314.

426 Unmuth, J. M. L., R. A. Lillie, D. S. Dreikosen, and D. W. Marshall. 2000. Influence of
427 dense growth of Eurasian Watermilfoil on lake water temperature and dissolved
428 oxygen. *J. Freshwater Ecol.* **15**: 497-503.

429 Van de Bogert, M. C., S. R. Carpenter, J. J. Cole, and M. L. Pace. 2007. Assessing
430 pelagic and benthic metabolism using free water measurements. *Limnol. Oceanogr.:*
431 *Methods* **5**: 145-155.

432 Van de Bogert, M. C., D. L. Bade, S. R. Carpenter, J. J. Cole, M. L. Pace, P. C. Hanson,
433 and O. C. Langman. 2012. Spatial heterogeneity strongly affects estimates of
434 ecosystem metabolism in two north temperate lakes. *Limnol. Oceanogr.* **57**: 1689-
435 1700.

436 Verpoorter, C., T. Kutser, D. A. Seekell, and L. J. Tranvik. 2014. A global inventory of
437 lakes based on high-resolution satellite imagery. *Geophys. Res. Lett.* **41**: 6396–
438 6402.

439 Winslow, L. A., J. A. Zwart, R. D. Batt, H. A. Dugan, R. I. Woolway, J. R. Corman, and
440 J. S. Read. 2016. LakeMetabolizer: an R package for estimating lake metabolism
441 from free-water oxygen using diverse statistical methods. *Inland Waters* **6**: 622-636.
442
443
444
445
446
447
448
449
450
451
452
453
454
455
456
457
458

459 **Acknowledgements**

460 Access to our study lake was granted by Förderverein Feldberg-Uckermärkische
461 Seen e.V. We thank Rüdiger Mauersberger for background information on the lake,
462 Thomas Hintze and Reinhard Hölzel for technical assistance, Sebastian Rudnick, Jörg
463 Lewandowski and Nils Meyer for providing groundwater data, and Georgiy Kirillin and
464 two anonymous reviewers for their instructive comments. We also thank Marianne
465 Graupe, Barbara Meinck, Steffi Meyer, Steffi Schuchort, Grit Siegert, and Robert Tarasz
466 for their assistance in laboratory and/or fieldwork. This study was part of the
467 TERRALAC project, financed by the Leibniz Association (WGL).

468

469

470

471

472

473

474

475

476

477

478

479

480

481

482 **Table 1.** Seasonality of calculated gross primary production (GPP) and related
 483 meteorological data (May 8th, 2010 to May 7th, 2011).

	Percentage of negative GPP values	Mean whole- lake GPP from diel-O ₂ curves, negatives included (g C m ⁻² y ⁻¹)	Mean whole- lake GPP from diel-O ₂ curves, negatives excluded (g C m ⁻² y ⁻¹)	Phytoplankton GPP from P-I curves (g C m ⁻² y ⁻¹)	Mean wind speed (m s ⁻¹)	Mean day- to- night air temp. diff. (°C)
Spring (Mar- May)	30	138 ± 49 (n = 54)	307 ± 44 (n = 38)	165 ± 7 (n = 55)	1.26 ± 0.05	6.4 ± 0.6 (n =24)
Summer (Jun- Aug)	40	99 ± 52 (n = 88)	422 ± 41 (n = 53)	476 ± 17 (n = 88)	1.08 ± 0.04	9.2 ± 0.4 (n = 88)
Fall (Sep- Nov)	32	119 ± 26 (n = 86)	232 ± 27 (n = 58)	142 ± 6 (n = 86)	1.14 ± 0.04	5.6 ± 0.4 (n =

						86)
Winter (Dec- Feb)	81	-33 ± 25 (n = 63)	263 ± 99 (n = 11)	0 (n = 64)*	NA	3.9 ± 0.4 (n =65)
Total	45	83 ± 21 (n = 291)	315 ± 22 (n = 160)	216 ± 12 (n = 293)	0.90 ± .03	6.5 ± 0.2 (n = 263)

484 * Due to snow and ice cover, with resulting light transmittance anticipated to be low,

485 wintertime phytoplankton GPP was estimated to be zero.

486

487

488

489

490

491

492

493

494

495

496

497

498 **Figure captions**

499

500 **Figure 1.** Convective flow of oxygen from littoral to pelagic lake zones (black arrows)
501 above and parallel to the thermocline (dashed line) due to differential heating during the
502 day and differential cooling at night (adapted from Monismith et al. (1990) and Oldham
503 and Sturman (2001)). When coupled with higher primary production in the littoral zone
504 during the day and higher respiration at night, this convective flow may explain
505 unexpected oxygen curves measured at a central probe (such as rising overnight oxygen
506 concentrations).

507

508 **Figure 2.** Theoretical diel oxygen curves, showing higher primary productivity in the
509 littoral zone than the pelagic zone, and the resulting offset under advective current
510 conditions.

511

512 **Figure 3.** Sample oxygen measurements from Schulzensee (black circles), showing the
513 volumetric primary productivity rates (represented by the slopes of the solid and dashed
514 lines) which would result from the measured oxygen curves (solid lines, below measured
515 oxygen points), compared to independently determined phytoplankton production for the
516 same days (dashed lines, above oxygen points). Grey zones represent nighttime periods.

517

518 **Figure 4.** Full-year gross primary production of Schulzensee, as calculated from diel O₂
519 curves by LakeMetabolizer, comparing Bayesian, Kalman, bookkeeping, maximum-
520 likelihood estimation (MLE), and ordinary least squares (OLS) approaches. Boxes

521 represent the upper quartile, median, and lower quartile of values, with whiskers
522 representing the 5th and 95th percentiles. Centered squares represent the mean value, and
523 crosses designate minimum and maximum values in the dataset.

524

525

526

527

528

529

530

531

532

533

534

535

536

537

538

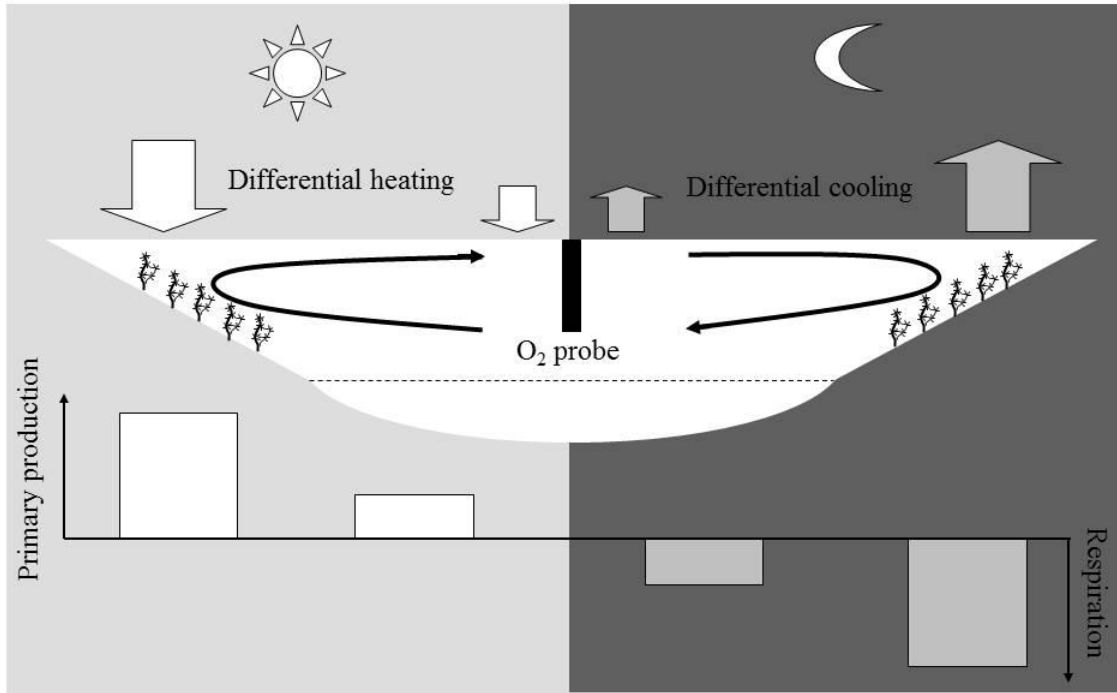
539

540

541

542

543



544

545 Fig. 1

546

547

548

549

550

551

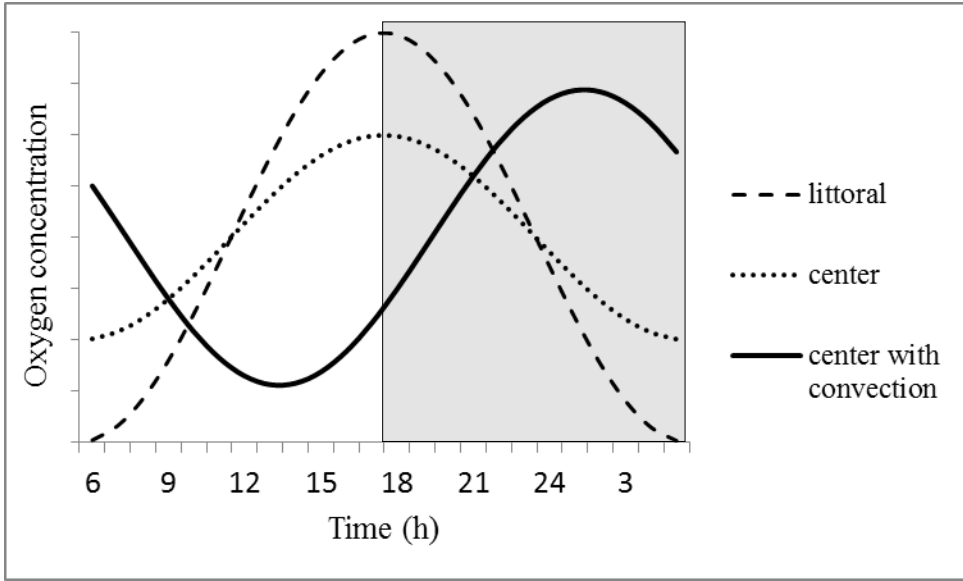
552

553

554

555

556



557

558

559 Fig 2.

560

561

562

563

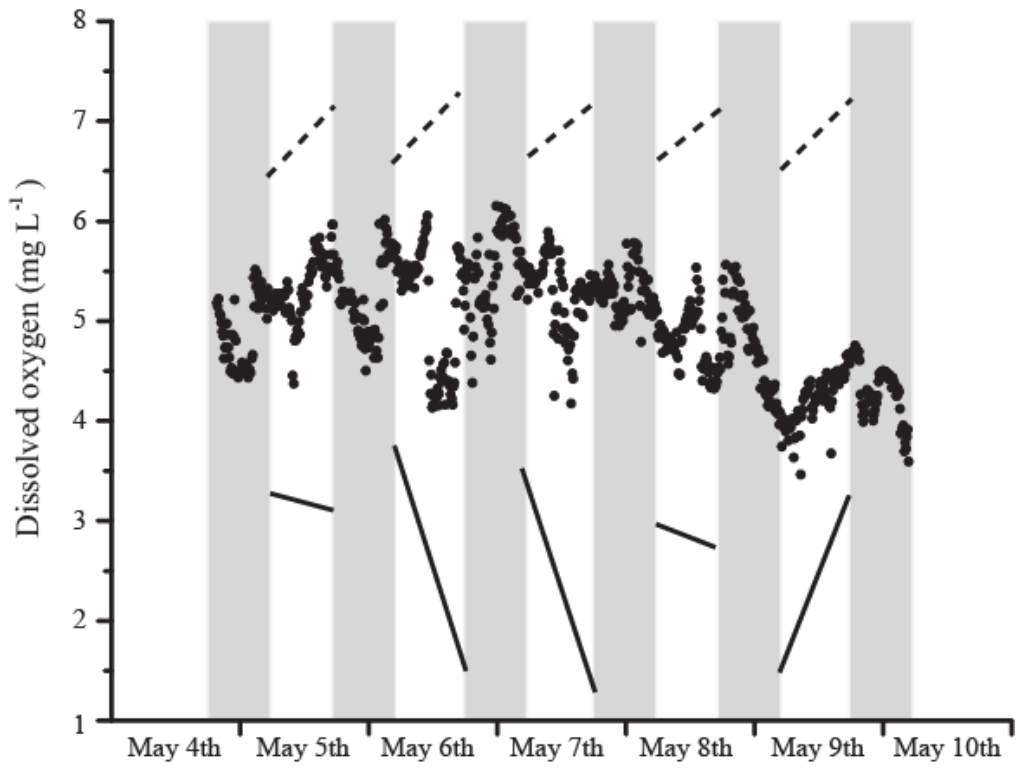
564

565

566

567

568



569

570

571 Fig. 3

572

573

574

575

576

577

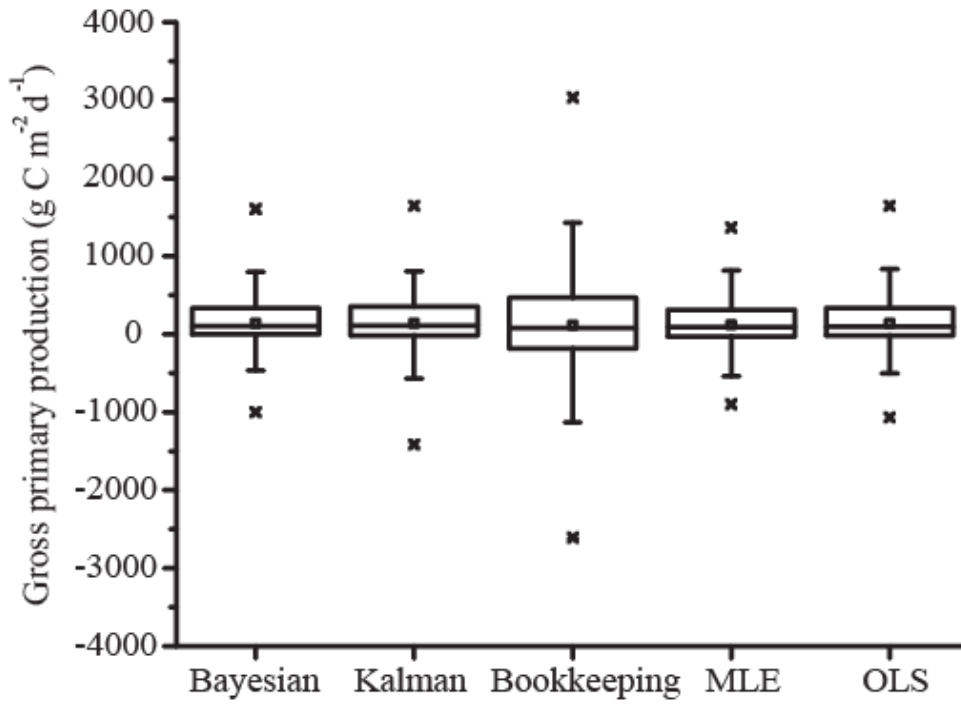
578

579

580

581

582



583

584

585 Fig. 4